GA–A24673

DIAGNOSTICS FOR EDGE PEDESTAL RESEARCH

by
A.W. LEONARD

MAY 2004

DISCLAIMER

GA–A24673

DIAGNOSTICS FOR EDGE PEDESTAL RESEARCH

by
A.W. LEONARD

This is a preprint of a paper to be presented at the 15th High Temperature Plasma Diagnostics Conf., San Diego, California, April 19–22, 2004 and to be published in *Rev. Sci. Instrum.*

Work supported by
the U.S. Department of Energy
under DE-FC02-04ER54698

GENERAL ATOMICS PROJECT 30200
MAY 2004

ABSTRACT

Edge pedestal research in magnetic plasma confinement devices requires measurements which span multiple spatial and temporal scales and include a number of physical processes. Research seeks to optimize the height of the pedestal for maximum confinement, but to avoid large repetitive particle and heat loads in the divertor as a consequence of edge localized modes (ELMs). In this complex region, transport physics, fueling by neutrals, stability physics, and the physics of the self-driven bootstrap current all play key roles. To develop an understanding of the pedestal region, detailed physics measurements of the local gradients, neutral fueling, the turbulence spectra, and the magnetohydrodynamic (MHD) characteristics are needed with both fine spatial and temporal resolution. Finally, development of two-dimensional and three-dimensional imaging of the ELM evolution would greatly aid in understanding ELM transport.

I. INTRODUCTION

The edge H–mode pedestal in the tokamak is currently the subject of extensive research in the magnetic fusion community. The edge pedestal results from a narrow transport barrier near the last closed plasma flux surface after the H–mode transition [1]. The sharp gradients are in a narrow region, no more than a few percent of the minor radius, just inside the separatrix. Though small in extent, this region has significant implications for the performance of the plasma. Core plasma temperature profiles are often stiff resulting in a very strong dependence on the pedestal temperature [2]. The emergence of gyrofluid [3,4] and gyrokinetic [5,6] approaches to turbulence and transport modeling also predict a very strong influence of the pedestal on the core plasma confinement. These models predict that the target fusion gain for ITER can be obtained if a pedestal temperature near 4 keV is achieved [7].

The edge pedestal can also create severe consequences for plasma facing components. As the profile gradients build in the pedestal, magnetohydrodynamic (MHD) stability limits can be approached, resulting in an instability known as an edge localized mode (ELM) [8]. The energy and particles released by an ELM onto the open field lines of the scrape-off-layer (SOL), quickly flow by parallel transport, and cause a short intense heat flux onto the divertor target. If the ELM is too large, the transient heat flux can exceed the surface material ablation threshold, with the potential to shorten the divertor target lifetime in a large tokamak such as ITER to a few discharges [9,10].

Due to the issues described above, current research seeks to optimize the height of the pedestal for maximum confinement, while simultaneously searching for ELM–free, or small ELM regimes which avoid large repetitive particle and heat loads in the divertor as a consequence of ELMs. In this complex region transport and neutral fueling physics, the physics of the self-driven bootstrap current, stability physics and non-linear evolution of the ELM instability, all play key roles. This paper describes the physical measurements that will be needed to study these processes with the goal of predicting and controlling the pedestal characteristics in future large tokamaks. Measurement needs that require additional diagnostic development will be particularly highlighted. In Section II measurement requirements for transport analysis and modeling are described. In Section III measurements to validate MHD stability models are discussed. In Section IV efforts to follow ELM evolution are presented. Finally in Section V the diagnostic development that is needed for future progress is discussed.

II. PEDESTAL TRANSPORT

The H–mode pedestal is formed due to a reduction in transport just inside the plasma's last closed flux surface. After the H–mode transition the height of the pedestal rises as the gradients increase and/or the transport barrier widens, until a stability limit is approached. To determine the level of transport in the pedestal not only are accurate measurements of the density and temperature profiles needed, but also the energy and particle sources driving the gradients in the profiles must be measured. Proceeding from characterizing the transport to testing our understanding, the measured transport levels can then be compared to theoretical models and simulation codes. An additional important comparison of experiments with the models is the characteristics of the turbulent fluctuations driving transport in the pedestal.

Profile measurements of density and temperature in the edge require both high spatial and temporal resolution. The pedestal width is typically only 1%–2% of the plasma minor radius, thus requiring better spatial resolution than the central plasma. On MAST, high spatial resolution is obtained with a Thomson scattering that employs ~300 measurement locations, Fig. 1, but the ruby laser only allows a single pulse per discharge [10]. On DIII–D the multi-pulse Thomson system uses closer detector spacing for the pedestal than the core plasma in keeping the number of channels to a moderate number [12].

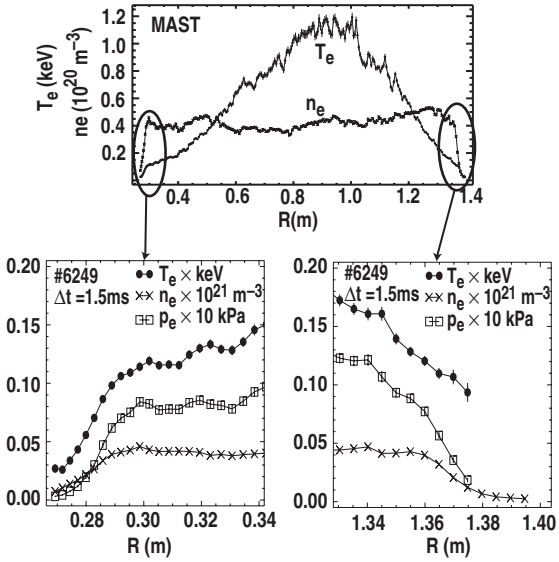

Fig. 1. Electron density and temperature profile from the MAST spherical tokamak using ~300 measurement locations across the plasma cross section. The inboard and outboard midplane pedestal profiles are expanded to show detail.

Another option for better spatial resolution is to align the Thomson laser more tangential to the plasma pedestal poloidal cross section. This has been successfully applied to resolve the pedestal profile in JET and ASDEX–Upgrade discharges [13]. One drawback of this approach is that plasma equilibrium shape required to achieve this tangential view can be quite restrictive.

Because the pedestal profiles evolve from one ELM to the next a temporal resolution approaching 1 ms is needed for typical ELM frequencies up to 100 Hz. Though the Thomson scattering measurements are made with a very short integration time, <1 μs, the limited repetition rate of the laser systems makes it difficult to follow the temporal evolution between more rapid ELMs. One approach around this limitation is to collect data during constant conditions over a number of ELM cycles and then reorder the data in time to reconstruct the time dependence of the profile from one ELM to the next [14].

Another useful diagnostic tool for the pedestal density profile is microwave reflectometry. An example of the pedestal density profile obtained by reflectometry on DIII–D is shown in Fig. 2. Recent advances in microwave techniques have enabled measurement of the density profile from the far SOL to the top of the pedestal with good temporal resolution of <25 μs for a complete profile [15,16]. For electron temperature, ECE can provide accurate high time resolution data for at least part of the pedestal. Except for high density tokamaks such as Alcator C–Mod, the ECE emission is typically no longer black-body in the lower density part of the pedestal and its interpretation is difficult. For this reason Thomson scattering remains the most useful measurement of the pedestal electron temperature profile.

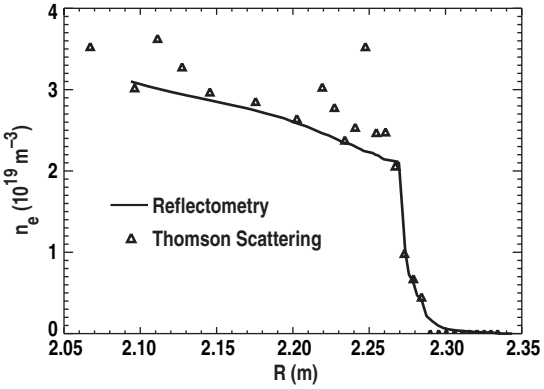

Fig. 2. The pedestal density measured by microwave reflectometry on DIII–D. Good agreement is obtained between the reflectometry and Thomson scattering diagnostics.

Ion temperature profiles are typically provided by charge exchange recombination spectroscopy systems (CER). By charge-exchange with background impurity ions this diagnostic provides the temperature of impurity ions as well as their density. By assuming rapid equilibration between main and impurity ions and subtracting the impurity density both the main ion density and temperature can be obtained. An example

of the evolution of the pedestal ion temperature profile obtained on JT–60U with CER is shown in Fig. 3 [17,18]. A pedestal CER system based on lithium beam injection has been developed on ASDEX–Upgrade and is now providing pedestal ion temperature profiles [19]. On DIII–D improved measurement instrumentation has allowed ion temperature measurement times of less than 300 μs while obtaining high spatial resolution of ≤0.5 cm by slowly sweeping the pedestal plasma past the detector views [20,21].

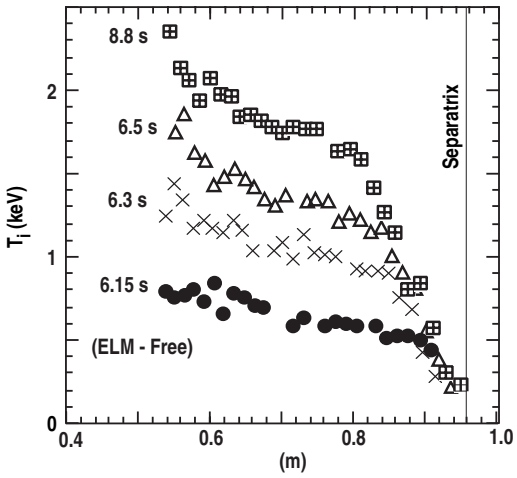

Fig. 3. The pedestal ion temperature profile measured by CXRS on JT–60U. The different profiles show an expansion of the pedestal through the discharge.

To determine the transport level in the pedestal, the sources of energy and particles that drive the pedestal gradients must also be determined. For the energy this measurement is usually straightforward as essentially all of the ohmic and auxiliary heating is deposited in the central plasma and then flows through the pedestal region. Measurements of the radiated power profile and charge-exchange losses typically account for only small adjustments to the pedestal energy flux. Particle sources driving the density gradient, on the other hand are expected to be significant within the pedestal itself. In addition, recent work has shown that it is also important to determine the poloidal profile of neutral particle fueling inside the separatrix as it may be an important factor in setting the pedestal density width [22].

Determining the 2D neutral particle source profile can be particularly difficult. In principle the neutral density, and resulting ionization rate, can be determined by measuring the local D_α emissivity and then calculating the ionization per photon efficiency from the measured electron density and temperature profiles. But in practice the D_α emissivity is usually hollow, peaked outside the separatrix, with strong poloidal asymmetry making inversion of 2D chord integrated measurements very uncertain. Additional complications include the possibility of toroidal asymmetries and D_α reflection from surfaces. Finally converting emission to ionization requires measurement

of the plasma temperature and density throughout the measurement region.

One approach to analysis of D_α measurements is to model the edge plasma and neutral flux in reproducing the D_α measurement. In this case the plasma profiles must be fit with measurements and/or modeling over the region of interest and the D_α signal inverted to obtain the local emissivity. This technique has been applied in 1D at the outer midplane on DIII–D [23] and Alcator C–Mod [24].

Expanding this type of analysis from 1D at the mid plane to complete 2D profiles becomes much more difficult with large uncertainties. Most significantly inverting the chord-averaged signals to the local 2D D_α emissivity profile is extremely difficult because of the hollow profile and strong poloidal asymmetry. Additionally the complete 2D profile, inside and outside the separatrix, is needed across the plasma cross section. Some useful neutral density measurements have been made near the X–point in DIII–D [25], but the spatial coverage is limited and the uncertainty large.

Initial investigations on ASDEX–Upgrade have had success in reproducing measured density and non-inverted D_α profiles by modeling the entire pedestal and SOL plasma with a fluid code and the neutrals with a 2D Monte Carlo code [13]. This type of combined measurement and modeling is likely to be required to make progress in understanding the role of the neutral profile on the pedestal density formation.

Pedestal research also seeks to understand the underlying mechanisms of radial transport in order to more reliably predict the pedestal gradients and widths in future devices. An important step in this direction will be to apply to the pedestal the gyrofluid and gyrokinetic codes that have been successful in modeling core plasma transport [2–7]. In addition to plasma profiles and particle and energy sources, comparisons to these models require an accurate description of the magnetic topology, particularly the magnetic shear. Efforts to measure the magnetic shear, or equivalently the toroidal current, in the pedestal are now under development and are described in the next section on pedestal stability. Another important aspect of the models is the role of sheared $E \times B$ flow in suppressing turbulent transport. Details of the radial electric field, its width and magnitude are provided by force balance considerations of CER measurements of impurity temperature, density and rotation. Another option implemented on ASDEX–Upgrade determines the pedestal radial electric field through Doppler reflectometry measurements of plasma fluctuation rotation perpendicular to the magnetic field [26].

The transport models also predict characteristics of the turbulence driving the transport. The width of the region of turbulence suppression is particularly important for predicting pedestal characteristics. Comparisons with fluctuation diagnostics have been used to validate the physics of the models for ion driven transport in the core plasma. Similar application of fluctuation diagnostics need to be applied to the pedestal. An

example of fluctuation data obtained from beam emission spectroscopy (BES) is shown in Fig. 4 [27,28]. In this figure BES captures 2D density fluctuations in the pedestal which significantly decrease at the onset of the H–mode phase. This type of data can provide the magnitude and frequency spectrum of the turbulence in both L–mode and H–mode as well as the extent of turbulence suppression in H–mode. Additional density fluctuation diagnostics which include microwave reflectometry and far infrared scattering should also be applied to the pedestal [29,30]. As theoretical models develop measurements of other fluctuating quantities, such as ion and electron temperatures even the turbulent fluxes through the pedestal, may also be required for transport studies.

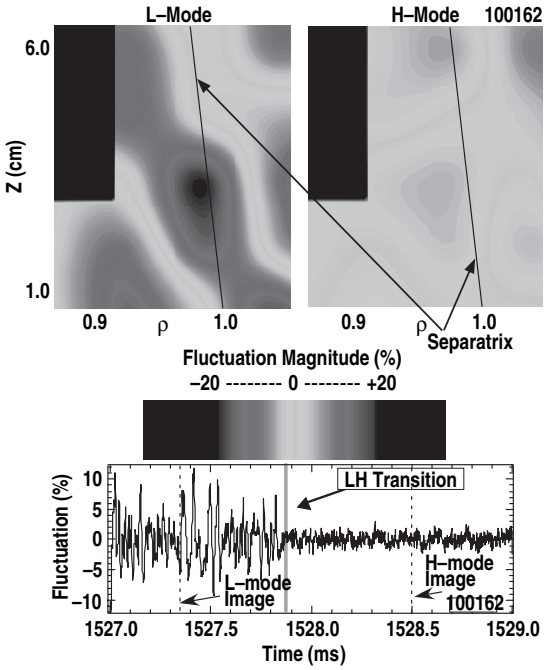

Fig. 4. Density fluctuation data from BES on DIII–D. The upper figures show the 2D density fluctuation pattern in L–mode on the left and H–mode on the right. The bottom time trace shows a single channel's fluctuation level drop at the transition to H–mode.

As an example of theoretical development driving diagnostic needs, modeling and simulation of transport is now includes electron dynamics [31]. The role of electron fluctuation driven transport is expected to be particularly important in the pedestal region and may represent the dominant energy transport process after the H–mode transition has suppressed ion driven turbulence. Validating the role of electron transport will require measuring turbulence at much shorter wavelengths. Most current fluctuation diagnostics, are limited to the longer wavelengths of ion driven turbulence. Efforts now underway to develop short wavelength fluctuation measurements include Phase Contrast Imaging (PCI) [32] and microwave scattering diagnostics [33]. Though this diagnostic development effort is aimed at core plasma measurements, designing flexibility into the

systems to allow measurements in the pedestal could be of particular value. Also, developing measurements of other fluctuating parameters may become more important as our models and understanding of transport in the pedestal improves.

III. PEDESTAL STABILITY

After the H–mode transition the pedestal gradients and/or width grows until the pedestal pressure is ultimately limited by MHD stability, typically by an ELM. In addition, the pedestal gradients can drive a strong edge current due to the bootstrap effect [34], which also plays an important role in edge stability. The edge current is a source of free energy that can drive external kink, or peeling modes, but the edge current also reduces magnetic shear in the pedestal, stabilizing higher–n ballooning modes, allowing higher pressure gradients before onset of the instability [35,36]. Pedestal MHD stability to these pressure and current gradients has been well described by a coupled peeling-ballooning model [34,35].

Validation of the peeling-ballooning model requires accurate measurement of the profiles driving the instability as well as the magnetic equilibrium that stabilizes it. Determination of the pressure profile is generally made by measurements of the electron temperature and density, and ion and impurity densities and temperatures as described in the earlier section on transport analysis. For stability analysis a few other issues must be considered as well. First, to test stability models the pressure gradient profile is needed just before the onset of an ELM. This requires sufficient time resolution in all of the profile measurements to follow the pressure gradient in the pedestal from ELM to ELM.

Another important aspect for experimental data is that pedestal stability is very dependent on the location of the separatrix with respect to the pressure profile. The degree of error in separatrix location varies across tokamaks depending on such uncertainties as magnetic sensor location and orientation, or toroidal asymmetries. While improvements to the magnetics measurements may be difficult and costly, these limitations can be overcome somewhat by adjustments to the magnetic equilibrium based upon physical arguments. For example, modeling of the edge radial and parallel power flux just outside the separatrix has found consistent solutions for the separatrix located on a characteristic part of the electron temperature profile [39]. Adjustments of the separatrix location in this manner allows for stability analysis across a wider set of data in a more consistent fashion. Any experimental constraints on separatrix location that could be developed through novel diagnostic techniques would be of significant aid in stability analysis.

The peeling-ballooning model also predicts the toroidal mode number for the onset of the ELM instability. Confirmation of the mode number at ELM onset would greatly aid in validating the model. ELM precursors have been observed on JET in magnetic probes and ECE, that are consistent with the mode numbers predicted by such a model [40]. Also consistent with the model, on DIII–D lower toroidal mode numbers, 5–10, have been observed with magnetic sensors at low density, while at high density higher mode

numbers, up to 30, are observed on reflectometry and BES [41]. However, mode numbers for the initial onset of the ELM, are not universally observable. The lack of mode number observation arises at least in part due to the high growth rate of the mode compared to the observable frequency, and also the nonlinear evolution of the mode. Better observations of the ELM onset will require development of fast diagnostics, to nearly 1 μs, which are more sensitive to low amplitude high order perturbations of the pedestal plasma.

Finally pedestal stability analysis requires accurate measurement of the local current density near the separatrix. The important part of this edge current is the bootstrap current which arises due to gradients in density and temperature. A direct measurement of the edge bootstrap current is needed not only for test of the stability models, but also for a test of the bootstrap current models themselves. The existing bootstrap models make assumptions that may be suspect for conditions in the pedestal, such as high collisionality, gradient scale lengths of the same order as the ion poloidal gyroradius, and radial electric fields which affect the ion banana orbits. An assessment of how these conditions may affect the pedestal bootstrap current is needed for reliable prediction of pedestal stability in future devices.

Measurements of the pedestal bootstrap current have been inferred through equilibrium reconstruction using external magnetic probes [42,43]. This type of analysis has indicated a total pedestal bootstrap consistent with bootstrap models, though the uncertainty in the current measurement is larger than needed to adequately validate the models. Also the spatial distribution of the bootstrap current cannot be adequately inferred from such equilibrium reconstruction analysis. For these reasons it is highly desirable to make very localized direct measurements of the magnetic field line pitch angles in the pedestal.

Local measurements of magnetic field line pitch angles have been reliably made using the motional Stark effect (MSE), where the Stark-split emission from a heating, or diagnostic beam is polarized with respect to the magnetic field direction. Diagnostics based upon MSE have been very successful in providing constraints for more accurate equilibrium reconstruction and determining the current profile over the bulk of the core plasma profile. While magnetic field line pitch angle measurements have been reliably made in the core plasma using the motional Stark effect, interpretation of MSE data is problematic in the pedestal because the strong radial electric field significantly affects the local current density measurement [43].

To overcome the ambiguity of MSE measurements in the pedestal, an edge current diagnostic based upon Zeeman polarimetry of an injected Lithium beam is now under development [44]. Because the Zeeman splitting is driven by the magnetic field in the lithium ion's reference frame, the pedestal electric field does not significantly affect the polarization angle of emission. Other advantages of this method include high spatial resolution and sufficient emissivity for strong signals. Preliminary measurements of field

line pitch angle and the edge current in the outer midplane pedestal from this diagnostic are shown in Fig. 5 [45]. This data, though preliminary, clearly shows the affect of the pedestal pressure gradient on the pitch angle profile and the edge toroidal current calculated from that profile. The edge current at the outer midplane is comprised of both the bootstrap and Pfirsch-Schlüter currents. A field line angle measurement accuracy of ≤1 deg will likely be required to separate these currents and adequately test the bootstrap current models. Improving accuracy and time resolution is a remaining challenge for edge current profile measurement.

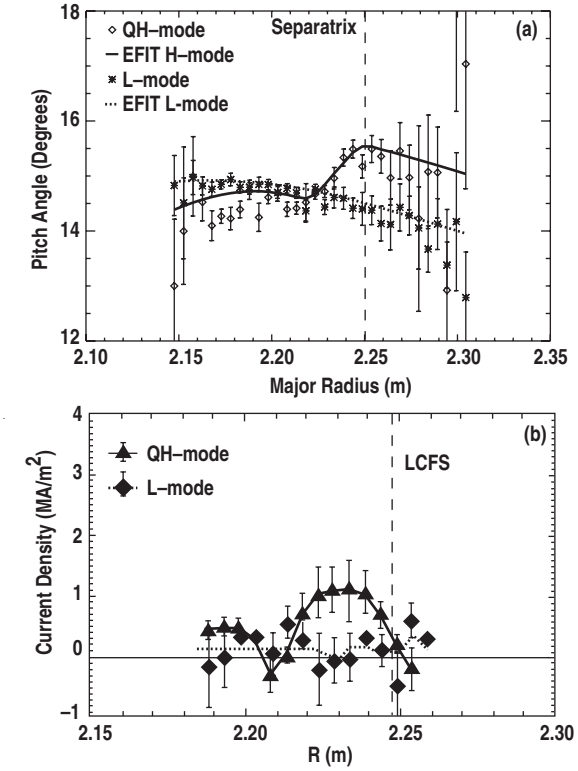

Fig. 5. Lithium beam polarimetry measurement in DIII–D of (a) the pitch angle profile at the outer midplane for L–mode and QH–mode. Also shown is the expected pitch angle profile from equilibrium reconstruction using the measured pressure gradient. (b) The current profile calculated from the pitch angle gradient for the same L–mode and QH–mode discharges.

IV. ELM DYNAMICS

The ELM instability is also a focus of pedestal research because of the its potential for damage to vessel components [9,10]. If an ELM releases too much energy from the pedestal into the SOL rapid parallel transport can lead to excessive heating and erosion of the divertor target, or other plasma facing surfaces. Understanding and predicting the characteristics of the ELM energy release will be a key in designing operational scenarios that will be compatible with long divertor component lifetime. As a first step toward this understanding, the released ELM energy has been compared with the width of the most unstable peeling-ballooning eigenmode just before the onset of the ELM instability [46]. Though a generally positive correlation has been found with this approach, it does not take into account the nonlinear evolution and interaction of multiple mode numbers, nor describe the underlying ELM transport. In addition operational regimes in H–mode with no ELMs, or very small ELMs, have been observed that cannot be fully explained by this approach. An understanding of the ELM evolution and transport will be required to reliably predict ELM size and benign ELM regimes in future large tokamaks.

Experimental observations of ELM evolution and transport can guide and validate theoretical work on these topics that is just now getting underway [47]. A full experimental description of an ELM, however, will be quite a challenge. The ELM perturbation to pedestal density and temperature profiles takes place on the μsec time scale with small scale spatial features that are very irregular spatially and temporally. Initial measurements of pedestal density fluctuations with BES indicate perturbations with a characteristic size of about 1 cm that propagate both toroidally and radially during an ELM. However, current implementations of BES only cover a small cross section, 3×5 cm, of the entire poloidal extent of the pedestal. Measurements from ECE may also provide some information about the electron temperature perturbation, but are also lacking in providing 2D information.

With a lack of pedestal diagnostics to describe ELM evolution and transport boundary diagnostics of the SOL and divertor may provide some insight into the ELM instability dynamics. As a simple example, Fig. 6, an image of an ELM was captured in the MAST spherical tokamak by using a short integration time, visible camera [48]. Though qualitative in nature, several important ELM features can be confirmed by such an image. The ELM perturbation is a filamentary-like structure, bulging out on the outboard side. Also the toroidal mode number appears to be of a moderate range between 10 and 20. Such images can help guide further theoretical and experimental work. Other SOL diagnostics can produce more quantitative, though more local, information on ELM dynamics. On JT–60U [49] and ASDEX–Upgrade [50] microwave reflectometry confirms the density perturbation occurs first at the outer midplane while the density

perturbation propagates to the inboard pedestal at the ion sound speed. Fast microwave reflectometry has been used on DIII–D to measure the radial propagation speed of the ELM density perturbation into the SOL at nearly 1 km/s [49]. Insertable Langmuir probes have been used on JET [52] and DIII–D [51] to measure a large electron density and high electron temperature, similar to the pedestal, in the ELM perturbation that diffuses as it propagates radially in the SOL. These kind of data can be used to determine radial particle fluxes due to an ELM as well as characteristics of the transport processes. Diagnostics at the divertor target can also add insight into ELM dynamics and transport. The time behavior of particle fluxes and electron temperatures measured by Langmuir probes fixed in the divertor target can indicate different transport processes that are occurring during an ELM. Measurements with an IR camera in ASDEX–Upgrade exhibit a 2D striation pattern during an ELM that is consistent with a SOL perturbation with toroidal mode numbers of 8 to 24 [53].

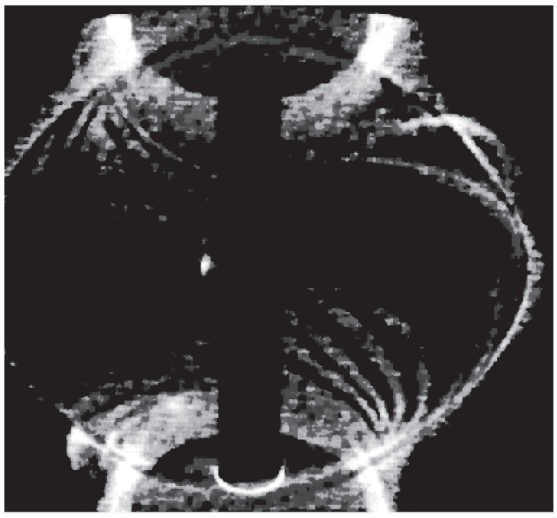

Fig. 6. A camera image in visible light of the MAST spherical tokamak capturing an ELM.

V. DISCUSSION

There is clearly further diagnostic development work needed to advance research on the tokamak edge H–mode pedestal. In particular, improvements are needed in each of the physics topics described; transport, MHD stability and ELM evolution and transport. These diagnostic needs are summarized in Table I.

TABLE I.

Physical Measurement	Diagnostic	Desired Improvements, Comments
Transport		
Plasma profiles	Thomson, CER, reflectometry, ECE, etc.	Spatial and temporal resolution
Neutral 2D profile	D_α with modeling	Large uncertainty, critical need
Radial E field	CER, Doppler reflectometry	Available, improving
Turbulence	BES, PCI, microwave scattering	Shorter wavelength measurements
MHD Stability		
Equilibrium reconstruction	Magnetic probes	Higher accuracy, toroidal asymmetries
Pressure profile	Plasma profile diagnostics	Available
Current profile	Lithium beam polarimetry	Spatial and temporal resolution
ELM mode number at onset	Magnetic probes, BES, reflectometry	More sensitivity to high mode numbers
ELM Dynamics		
ELM evolution	BES, SXR	Fast 2D imaging of pedestal plasma
ELM transport	SOL probes, reflectometry	More spatial coverage

For characterizing transport, improvements in spatial and temporal resolution of pedestal profile measurements are certainly desirable, but this should be simply a matter of providing additional resources for already proven techniques. But, measuring the particle source in the in the pedestal is also critical for characterizing and modeling transport, and it is likely to be the most difficult challenge for pedestal diagnostics. Because of the strong ionization source outside the pedestal, in the SOL and divertor obtaining this profile can be very complicated. Significant 3D asymmetries and reflections further complicate the measurement. Progress has been made with analysis of either tangential camera images of D_α, or multiple arrays of multi-chord D_α photo-detectors coupled with edge plasma and neutral modeling. This is an area where pedestal and boundary research overlap and collaboration could prove fruitful for both topics. However, additional diagnostic development to directly measure the 2D neutral density profile inside the separatrix would still be of great benefit.

Finally as our understanding of transport in the pedestal improves there will be an increasing desire to measure the underlying turbulence driving that transport. At this time fluctuation diagnostics developed for core plasma transport studies can be applied to the pedestal region. However as our understanding of the unique aspects of the pedestal transport improves fluctuation diagnostic development specifically for the pedestal will likely be required.

There has been encouraging progress in measuring the edge toroidal current density for MHD stability analysis. But further progress is needed and achieving it will require a continuing dedicated effort. The payoff for this effort will not only be a critical test of edge stability, but also validation of the edge bootstrap models. Without a validated pedestal bootstrap current model, predictions of pedestal parameters and behavior in a future large tokamak will remain uncertain. Due to the critical nature of the edge current it seems warranted to pursue its measurement on additional tokamaks.

Finally diagnostic development is needed for studying the ELM instability itself. This will not be easy as the ELM is a fast chaotic process with a complicated fine spatial structure. New techniques will be needed to describe, or image, the evolution of its spatial structure within the pedestal. While, theoretical work on the nonlinear evolution of the ELM perturbation is just beginning, only experimental data can provide the insight that is needed in developing an ELM transport model.

REFERENCES

[1] F. Wagner, G. Becker, K. Behringer, *et al.,* Phys. Rev. Lett. **49**, 1408 (1982)

[2] J.E. Kinsey, T. Onjun, G. Bateman, A. Kritz, A. Pankin, G. Staebler, and R.E. Waltz, Nucl. Fusion **43**, 1845 (2003).

[3] M.A. Beer and G.W. Hammet, Phys. Plasmas **3**, 4046 (1996).

[4] R.E. Waltz, G.M. Staebler, W. Dorland, G.W. Hammett, M. Kotschenreuther, and J.A Konings, Phys Plasmas **4**, 2482 (1997).

[5] R.D. Sydora, Phys. Scr. **52**, 474 (1995).

[6] A.M. Dimits, T.J. Williams, J.A. Byers, and B.I. Cohen, Phys. Rev. Lett. **77**, 71 (1996).

[7] J.E. Kinsey, G.M. Staebler, and R.E. Waltz, Fusion Sci. and Tech. **44**, 763 (2003).

[8] E.J. Doyle, R.J. Groebner, K.H. Burrell, P. Gohil, T. Lehecka, N.C. Luhmann, Jr., H. Matsumoto, T.H. Osborne, W.A. Peebles and R. Philipona, Phys. Fluids B **3**, 2300 (1991).

[9] A.W. Leonard, A. Herrmann, K. Itami, J. Lingertat, A. Loarte, T.H. Osborne, W. Suttrop, the ITER Divertor Modeling and Database Expert Group, the ITER Divertor Physics Expert Group, J. Nucl. Mater. **266–269**, 109 (1999).

[10] G. Federici, P. Andrew, P. Barabashi, J. Brooks, R. Doerner, A Geier, A. Herrmann, G. Janeschitz, K. Krieger, A. Kukushkin, A. Loarte, R. Neu, G. Saibene, M. Shimada, G. Strohmayer, M. Sugihara, J. Nucl. Mater. **313–316**, 11 (2003).

[12] M.J. Walsh, E.R. Arends, P.G. Carolan, M.R. Dunstan, M.J. Forrest, S.K. Nielsen and R. O'Gorman, Rev. Sci. Instrum. **74**, 1663 (2003).

[13] A. Kallenbach, Y. Andrew, M. Beurskens, G. Corrigan, T. Eich, S. Jachmich, M. Kempenaars, A. Korotkov, A. Loarte, G. Matthews, P. Monier-Garbet, G. Saibene, J. Spence, W. Suttrop and JET EFDA Contributors, Plasma Phys. Control. Fusion **46**, 431 (2004).

[14] A.W. Leonard, R.J. Groebner, M.A. Mahdavi, T.H. Osborne, M.E. Fenstermacher, C.J. Lasnier and T.W. Petrie, Plasma Phys. Control. Fusion **44**, 945 (2002).

[15] L. Zeng, E.J. Doyle, T.L. Rhodes, G. Wang, W.A. Peebles and K.H. Burrell, Rev. Sci. Instrum. **74**, 1530 (2003).

[16] G. Wang, this issue

[17] Y. Koide, A. Sakasai, Y. Sakamoto, H. Kubo and T. Sugie, Rev. Sci. Instrum. **72**, 119 (2001).

[18] Y. Kamada, T. Hatae, T. Fukuda, and T. Takizuka, Plasma Phys. Control. Fusion **41**, 1371 (1999).

[19] M. Reich, E. Wolfrum, J. Schweinzer, H. Ehmler, L.D. Horton, J. Neuhauser and ASDEX Upgrade Team, accepted for publication in Plasma Physic. Control. Fusion.

[20] K.H. Burrell, *et al.,* accepted for publication in Plasma Phys. Control. Fusion (2004).

[21] K.H. Burrell, *et al.,* this conference.

[22] R.J. Groebner, M.A. Mahdavi, A.W. Leonard, T.H. Osborne, N.S. Wolf, G.D. Porter, P.C. Stangeby, N.H. Brooks, R.J. Colchin, and L.W. Owen, Nucl. Fusion **44**, 204 (2004).

[23] R.J. Colchin, L.W. Owen, J. Nucl. Mater. **313–316**, 609 (2003).

[24] J. Hughes, submitted to J. Nucl. Mater.

[25] R.J. Colchin, R. Maingi, M.E. Fenstermacher, T.N. Carlstrom, R.C. Isler, L.W. Owen, R.J. Groebner, Nucl. Fusion **40**, 175 (2000)

[26] G.D. Conway, J. Schirmer, S. Klenge, W. Suttrop, E. Holzhauer and the ASDEX Upgrade Team, submitted to Plasma Phys. Control. Fusion.

[27] G.R. McKee, C. Fenzi, R.J. Fonck, M. Jakubowski, Rev. Sci. Instrum. **74**, 2014 (2003)

[28] G.R. McKee, R. Ashley, R. Durst, R. Fonck, M. Jakubowski, K. Tritz, K.H. Burrell, C.M. Greenfield, J.I. Robinson, Rev. Sci. Instrum. **70**, 913 (1998).

[29] W.A. Peebles, S. Baang, D.L. Brower, K.H. Burrell, E.J. Doyle, R.J. Groebner, T. Lehecka, N.C. Luhmann, Jr., H. Matsumoto, R. Philipona, C.L. Rettig, T.L. Rhodes, and C.X. Yu. Rev. Sci. Instrum. **61**, 3509, (1990).

[30] C.L. Rettig, W.A. Peebles, E.J. Doyle, K.H. Burrell, and R.J. Groebner, Phys. Plasmas **3**, 2374 (1996).

[31] J.E. Kinsey, G.M. Staebler, and R.E. Waltz, Phys. Plasmas **9**, 1676 (2002)

[32] J.C. Rost, this conference

[33] W.A. Peebles, T.L. Rhodes, X. Nguyen, L. Zeng, and M.A. Gilmore, this conference.

[34] O. Sauter, C. Angioni, and Y.R. Lin-Liu, Phys. Plasmas **6**, 2834 (1999).

[35] J.R. Ferron, M.S. Chu, G.L. Jackson, L.L. Lao, R.L. Miller, T.H. Osborne, P.B. Snyder, E.J. Strait, T.S. Taylor, A.D. Turnbull, A.M. Garofalo, M.A. Makowski, B.W. Rice, M.S. Chance, L.R. Baylor, M. Murakami, and M.R. Wade, Phys Plasmas **7,** 1976 (2000).

[36] T.H. Osborne, R.J. Groebner, L.L. Lao, A.W. Leonard, R. Maingi, R.L. Miller, G.D. Porter, D.M. Thomas, and R.E. Waltz Plasma Phys. Control. Fusion **40,** 845 (1998).

[37] J.W. Connor, R.J. Hastie, and H.R. Wilson, Phys. Plasmas **5**, 2687 (1998).

[38] P.B. Snyder, H.R. Wilson, J.R. Ferron, L.L. Lao, A.W. Leonard, T.H. Osborne, A.D. Turnbull, D. Mossessian, M. Murakami, X.Q. Xu, Phys. Plasmas **9**, 2037 (2002).

[39] G.D. Porter, J. Moller, M. Brown, and C.J. Lasnier, Phys. Plasmas **5**, 1410 (1998).

[40] C.P. Perez, H.R. Koslowski, G.T.A. Huysmans, T.C. Hender, P. Smeulders, B. Alper, E. de la Luna, R.J. Hastie, L. Meneses, M.F.F. Nave, V. Parail, M. Zerbini, and JET–EFDA Contributors, Nucl. Fusion **44**, 609 (2004)

[41] T.H. Osborne, A.W. Leonard, M.A. Mahdavi, M.S. Chu, M.E. Fenstermacher, R.J. La Haye, G.R. McKee, T.W. Petrie, E.J. Doyle, G.M. Staebler, M.R. Wade, and the DIII–D Team, Phys. Plasmas **8**, 2017 (2001).

[42] P.J. McCarthy, R.C. Wolf, J. Hobirk, *et al.,* Proc. 27th Euro. Conf. on Control. Fusion and Plasma Phys., Budapest, 2000, Vol. 24B (European Physical Society) p. 440.

[43] M.R. Wade, *et al.,* to be published in Phys. Rev. Lett. (2004).

[43] B.W. Rice, D.G. Nilson, K.H. Burrell, and L.L. Lao, Rev. Sci. Instrum. **70**, 815 (1999).

[44] D.M. Thomas, Rev. Sci. Instrum. **74**, 1541 (2003).

[45] D.M. Thomas, A.W. Leonard, H.W. Müller, submitted to Phys. Rev. Lett.

[46] A.W. Leonard, T.H. Osborne, M.E. Fenstermacher, R.J. Groebner, M. Groth, C.J. Lasnier, M.A. Mahdavi, T.W. Petrie, P.B. Snyder, J.G. Watkins, L. Zeng, Phys. Plasmas **10**, 1765 (2003).

[47] S.C. Cowley, H. Wilson, O. Hurricane and B. Fong, Plasma Phys. Control. Fusion **45**, A31 (2003).

[48] A. Kirk accepted for publication in Phys. Rev. Lett.

[49] N. Oyama, N. Asakura, A.V. Chankin, T. Oikawa, M. Sugihara, H. Takenaga, K. Itami, Y. Miura, Y. Kamada, K. Shinohara and the JT–60U Team, Nucl. Fusion **44**, 582 (2004).

[50] I. Nunes, G.D. Conway, A. Loarte, M. Manso, F. Serra, W. Suttrop, and the CFN and ASDEX–Upgrade Teams, accepted for publication in Nucl. Fusion.

[51] M.E. Fenstermacher, A.W. Leonard, P.B. Snyder, J.A. Boedo, N.H. Brooks, R.J. Colchin, D.S. Gray, R.J. Groebner, M. Groth, E.M. Hollmann, C.J. Lasnier, T.H. Osborne, T.W. Petrie, D.L. Rudakov, H. Takahashi, J.G. Watkins, L. Zeng and the DIII–D Team Plasma Phys. Control. Fusion **45**, 1597 (2003).

[52] B. Gonçalves, C. Hidalgo, M.A. Pedrosa, C. Silva, R. Balbín, K. Erents, M. Hron, A. Loarte, and G. Matthews, Plasma Phys. Control. Fusion **45**, 1627 (2003).

[53] T. Eich, A. Herrmann, J. Neuhauser, and the ASDEX Upgrade Team, Phys. Rev. Lett. **91**, 195003-1 (2003).

ACKNOWLEDGMENTS

This is a report of work supported by the U.S. Department of Energy under Cooperative Agreement DE-FC02-04ER54698. A number of individual contributed ideas, suggestions, figures and references for this paper. The author would like to thank K.H. Burrell, G. Conway, T. Eich, L.D. Horton, J.W. Hughes, A. Kallenbach, A. Kirk, A. Loarte, G.R. McKee, D. Mossessian, T.H. Osborne, T.L. Rhodes, P.B. Snyder, D.M. Thomas, and L. Zeng.